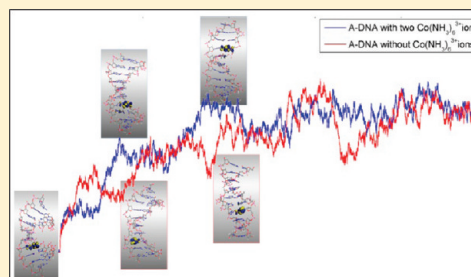


# Molecular Dynamics Study and Electronic Structure Evolution of a DNA Duplex d(CCCGATCGGG)<sub>2</sub>

Basab Chattopadhyay and Monika Mukherjee\*

Department of Solid State Physics, Indian Association for the Cultivation of Science, Kolkata 700032, India

**ABSTRACT:** The molecular dynamics simulations and electronic structure evolution of a A-DNA decamer, d(CCCGATCGGG)<sub>2</sub>, in the presence and absence of [Co(NH<sub>3</sub>)<sub>6</sub>]<sup>3+</sup> ions have been investigated. In both cases, the results of 2.5 ns MD simulation indicate a A-DNA → B-DNA transition. Ab initio DFT calculations were performed on a series of conformations representing the A → B transitions to reveal the dynamical behavior of the electronic structure of the decamer. The results suggest that the conformational parameters as well as the surrounding environment have no direct correlation with the electronic structures. Instead, the thermal fluctuations play an important role in the electronic structure of the present DNA system.



## 1. INTRODUCTION

The nucleic acid DNA molecules act as carriers of genetical information used in the development and functioning of most of the living organisms. Depending on the sequence, the amount and direction of supercoiling, chemical modifications of bases, and the ionic environment as well as the hydration conditions DNA molecules can exist in different conformations identified as forms A, B, C, etc.<sup>1</sup> The right-handed double helical B-DNA is, however, the most common form under the physiological conditions found in cells.<sup>2</sup> The conformation of the DNA molecule plays an important role in its biological functions, such as the interactions between DNA and protein, and DNA and RNA, and DNA transcription, etc.<sup>3,4</sup> Different conformations of DNA, even with the same sequence, can exhibit different electronic structures resulting in different conductance.<sup>5–10</sup> The electronic structure evolution accompanying the conformation transition process from one DNA form to another is also relevant to its chemical and biological functions.<sup>11,12</sup> The DNA damage and repair is known to be related to its charge-transfer properties, i.e., its electronic structure, specially its highest occupied molecular orbital (HOMO) and lowest unoccupied molecular orbital (LUMO) distributions.<sup>13,14</sup> It is also interesting from the point of view of nanotechnology to study the specific conformation that can determine the electrostatic structure and transport properties of DNA, which in turn can be effective in modulating the conductivity behavior of DNA nanowire.

Although several experimental biophysical techniques are available for studying femtosecond time-resolved charge-transfer phenomenon in DNA,<sup>15,16</sup> there is no experimental method capable of generating a complete description of the dynamic structure of DNA in its native environment, i.e., to evaluate the electronic structure of DNA during its conformational transition process or to trace DNA conformation transition trajectory. Molecular dynamics (MD) simulations can, in principle, provide a complete description of structural evolutions of DNA systems.<sup>17,18</sup> With the increase in computational power,

ab initio quantum mechanical calculations based on density functional theory can nowadays be used to investigate the electronic properties of DNA molecules.<sup>19</sup> Several ab initio calculations describing the electronic structures of DNA have been reported recently.<sup>5,6,14,20–22</sup> In most of these studies, a static DNA model was assumed; i.e., the DNA system was treated as one kind of periodic infinite crystal, which is certainly not a realistic situation in nature since DNA molecules are highly flexible. The time scale in some ab initio MD simulations of DNA was also not long enough to follow the conformation transition process.<sup>23</sup> Such an ab initio MD simulation is unlikely to yield a reliable dynamic trajectory because it cannot deal with the long-range interactions, which are very important for the stability of the DNA conformation. Cheatham and Kollman<sup>24</sup> had demonstrated that a classical MD simulation was highly effective in describing the conformation transition of DNA molecules. Classical MD simulations coupled with ab initio density functional calculations have been utilized to study the electronic structure evolution of DNA during its conformation transition process and to evaluate relationship between the DNA base pair stack and charge-transfer process.<sup>25–27</sup> The dynamics of the DNA structure and its impact on the electronic structure evolution during its fluctuation around the stable B-type conformation have been reported by Lewis et al.<sup>14</sup> Most of these studies were, however, limited to model DNA systems constructed using only two of the four DNA nucleotides.<sup>11,12,14</sup>

A combination of classical molecular dynamics simulations with an electronic structure density-functional method would be particularly useful in revealing the electronic states of a synthetic DNA system containing all four types of nucleotides (A, T, G, and C) present in a natural DNA, as the molecule undergoes conformational transition. For a reliable conclusion on conformational transition, the DNA duplex to be investigated should contain at least one helix turn, i.e., 10 base pairs, since smaller

**Received:** October 12, 2010

**Revised:** January 11, 2011

**Published:** February 3, 2011

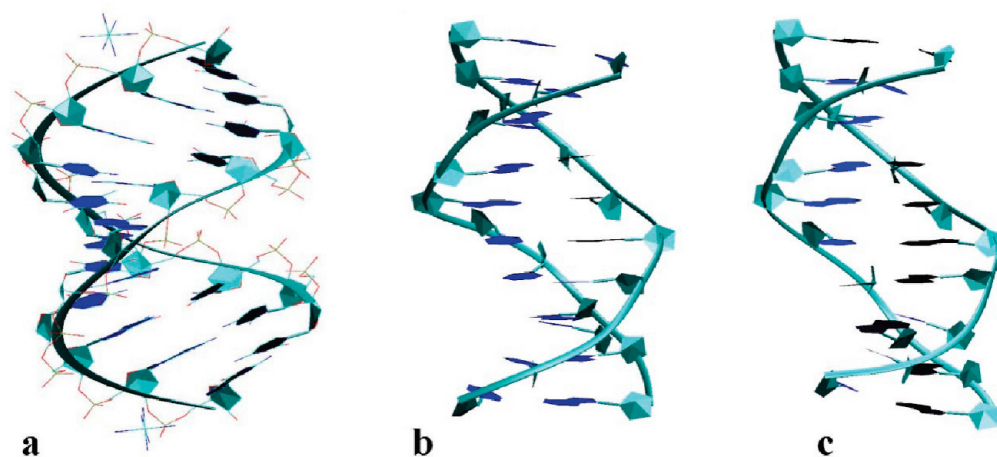


**Figure 1.** (a) Initial X-ray structure; (b) average structure corresponding to simulation A1; (c) average structure corresponding to simulation A2.

duplexes might not provide a good model of interactions along the major and minor grooves and would maximize the effect of artifactual end effects.<sup>28</sup> The decameric DNA duplex, d(CCCGATCGGG)<sub>2</sub>, satisfying the above criteria and for which a near-atomic resolution (1.25 Å) crystal structure is available,<sup>29</sup> was chosen as the simulation object with the aim to study the dynamics of DNA structure and its impact on the electronic structure evolution during conformation transition process. The crystal structure of the A-DNA used in the present analysis<sup>29</sup> contained two cobalt hexammine ions, which seem to promote the A-conformation of DNA molecules in the solid state.<sup>30</sup> It is known that cobalt hexammine ions have different binding modes for A-DNA duplex structures, either bridging the phosphate groups or adhering to edges of the adjacent guanines.<sup>31,32</sup> Crystallographic analysis of cobalt hexammine interaction with A-DNA duplex d(CCCGATCGGG)<sub>2</sub>, however, indicated only one kind of binding site involving the phosphate groups.<sup>29</sup> This is consistent with the electrostatic interaction between the negatively charged phosphate groups and the positively charged cobalt hexammine ion.

The present work reports a theoretical investigation of the electronic states of DNA decamer, d(CCCGATCGGG)<sub>2</sub>, with and without the cobalt hexammine ion pairs as the molecule undergoes form A → B conformation transition and classical thermal motion at room temperature by using a combination of molecular dynamics simulations and electronic structure density functional method. The analysis also allowed us to investigate the effect of cobalt hexammine ions on the dynamics of A-DNA structure during transition and their impact on the electronic structure.

## 2. THEORETICAL METHOD

**2.1. Classical MD Simulation.** Two classical MD simulations of DNA duplex d(CCCGATCGGG)<sub>2</sub> containing 10 base pairs (630 atoms) have been performed at a time scale of 2.5 ns using AMBER 8 package<sup>33,34</sup> in the presence (A1) and absence (A2) of cobalt hexammine ion pair (Figure 1). Simulation A1 started with the A-form of d(CCCGATCGGG)<sub>2</sub> containing a pair of cobalt hexammine ions (PDB id 1m77) while that of A2 used the same structure but without the ion pair. Standard AMBER parm99<sup>35</sup> force field was assigned. The following ion parameters were adopted for the cobalt hexammine ions: Co (radius 0.5 Å and well depth 0.01 kcal mol<sup>-1</sup>), N (radius 1.824 Å and well depth 0.17 kcal mol<sup>-1</sup>), and H (radius 0.6 Å and well depth 0.0157 kcal mol<sup>-1</sup>).<sup>36</sup>

Considering the overall electroneutrality of the system, an appropriate number of Na<sup>+</sup> ions (12 in A1 and 18 in A2) was added to the most electronegative areas around the decamers. Sodium ion concentration reaches a value of ~0.16 M in A1 and 0.21 M in A2. The ions were initially placed at sites with deepest electrostatic potential by using the XLEaP module of AMBER.<sup>34</sup> Parameters used for Na<sup>+</sup> ions were radius 1.868 Å and well depth 0.002 77 kcal mol<sup>-1</sup>.<sup>37</sup> The systems A1 and A2 were then solvated with 3157 and 3396 TIP3P water molecules,<sup>38</sup> respectively, to create a truncated octahedron box with a 8.0 Å buffer along each dimension. To avoid the edge effects, periodic boundary conditions were applied in all calculations.

The simulation protocols adopted were as follows. First, 1000 steps of energy minimization (500 steps of steepest descent followed by 500 steps of conjugate gradient) were carried out with harmonic restraints of 500 kcal mol<sup>-1</sup> Å<sup>2</sup> on the DNA followed by another 2500 steps of energy minimization (1000 steps of steepest descent followed by 1500 steps of conjugate gradient) without any restraint. For the equilibration, 10 ps heating up (from 0 to 300 K) and 10 ps equilibrating MD were performed initially with harmonic restraint of 10 kcal mol<sup>-1</sup> Å<sup>2</sup> on the DNA fragment using constant-volume and constant-temperature conditions, after which 200 ps unrestrained equilibration was carried out using a constant-pressure (1 atm) and a constant-temperature (300 K) conditions. The equilibration of both simulation processes was established by monitoring the system properties, i.e., density, volume, and pressure. Finally, 2300 ps production MD simulation was performed to obtain the A → B transition trajectory in both A1 and A2 systems. The temperature–bath coupling was achieved by the Langevin temperature equilibration<sup>39</sup> scheme using a collision frequency of 1.0 ps<sup>-1</sup> (with 0.2 ps coupling time). Long-range electrostatic interactions were treated using the particle-mesh Ewald (PME)<sup>40</sup> method with a cubic B-spline interpolations onto the charge grid with a spacing of ~1 Å and a 10<sup>-5</sup> tolerance for the direct space cutoff of 10 Å. The water models were held rigid, and the SHAKE algorithm<sup>41</sup> was applied to constrain all bonds to hydrogen with a tolerance of 10<sup>-5</sup> Å. The time step used for MD simulations was set to 2 fs. The equilibration protocol and runtime MD simulation parameters used here are somewhat dated, and a force field (parm99) known to have artifacts in the simulation of DNA over 10 ns time scale,<sup>42</sup> and imbalanced ion parameters.<sup>43</sup> Despite this, for simulations on the 2–3 ns time scale, the results are comparable to

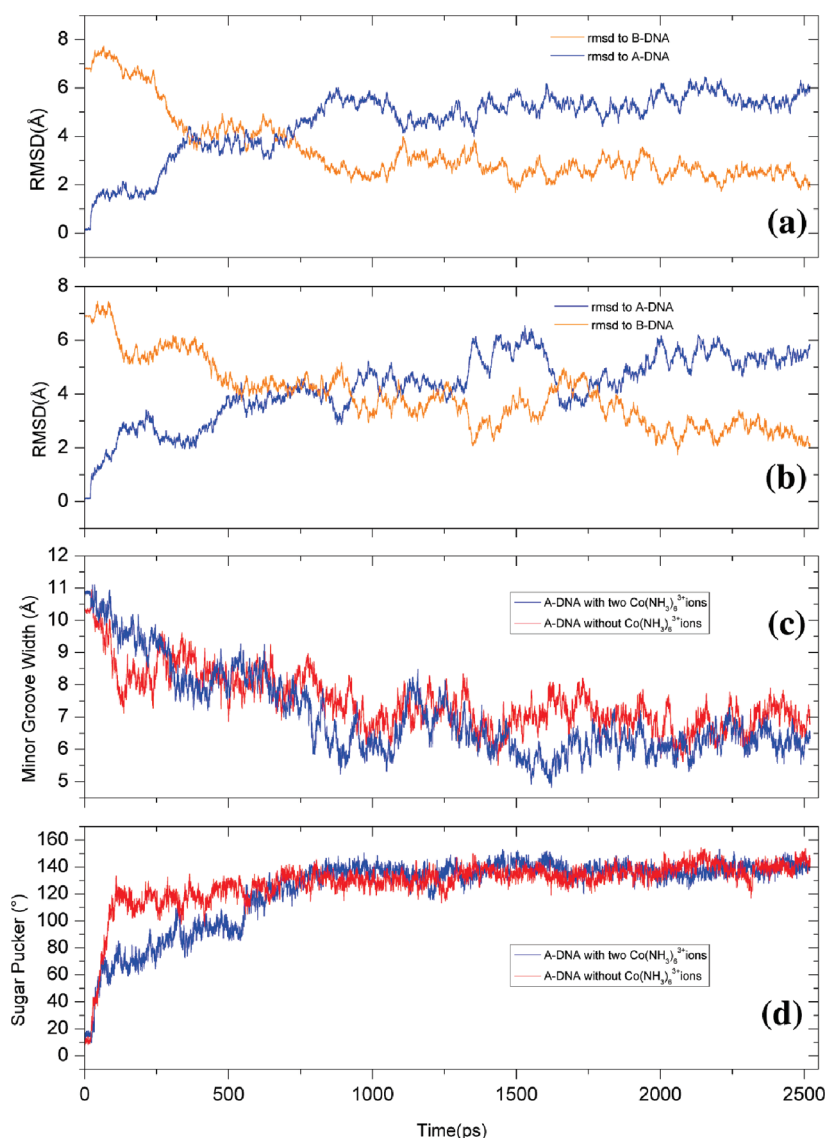


**Figure 2.** (a) Rmsds of simulation A1 with respect to the starting A-DNA (blue) and canonical B-DNA (orange); (b) rmsds of simulation A2 with respect to the starting A-DNA (blue) and canonical B-DNA (orange); (c) evolution of the average minor groove width (MGW) as a function of simulation time; (d) variation of the average sugar pucker (SP) as a function of simulation time.

more modern treatments<sup>44</sup> and have proven reliable for representing the DNA duplex structure.<sup>45,46</sup>

**2.2. Trajectory Analysis.** The sugar pucker (SP) and the minor groove width (MGW) were considered as two useful parameters to describe the DNA conformational character. Once the whole MD simulation trajectory was obtained, we used the ptraj program for analyzing the root-mean-squares deviation (rmsd) to evaluate the stability of the production run. We used the Curves program<sup>47</sup> to analyze the conformational parameters of all the snapshots obtained during the MD simulation, and then selected a few intermediate representative conformations. Besides the initial A-DNA, we selected five conformations that describe the A  $\rightarrow$  B transition process. Then, ab initio calculations based on the density functional theory were performed for these representative conformations to reveal their electronic structures.

**2.3. Electronic Structure Calculations.** A self-consistent density functional theory (DFT) calculation of the DNA structure of each snapshot was performed using the DMol<sup>3</sup> program package.<sup>48</sup> The DMol<sup>3</sup> program employs numerical basis functions

that are capable of describing long-range interactions. The single-point energy calculations for the representative conformations were performed using the DNP (double-numerical plus d and p-polarization functions to heavy atoms and hydrogens) basis set. The generalized gradient approximation (GGA)<sup>49</sup> by Perdew, Burke, and Ernzerhof (PBE)<sup>50</sup> was employed for the exchange–correlation functional. The GGA approximation was used instead of LDA (local density approximation) because it usually gives more accurate results for the electronic structure. The DNA was regarded as an oligonucleotide molecule, i.e., no periodic-boundary conditions were applied. After convergence of single-point calculations, the energy gaps were obtained and the molecular orbitals distributions of the systems were plotted.

### 3. RESULTS AND DISCUSSION

The energy and root-mean-squares deviation (rmsd) of all atoms in the DNA are usually used as indicators for judging the equilibrium of the system during MD simulation. The energy of



**Table 1.** Average Values of Minor Groove Width and Sugar Pucker for the Canonical A-DNA, Canonical B-DNA, the Reported X-ray Structure (PDB Code 1m77) of d(CCCGATCGGG)<sub>2</sub>, and the Average Structures of the Two Trajectories

	ADNA	BDNA	1m77	A1	A2
MGW (Å)	11.0	5.9	10(1)	4(2)	6(2)
SP (deg)	13.1	168.4	17(4)	141(25)	146(21)

simulations A1 and A2 is stable during the process, and the rmsd plots with respect to A-DNA and B-DNA are shown in Figure 2a, b. The transition from A-DNA toward B-DNA is visible during the first 500 ps of the production simulation. Similar to earlier studies,<sup>12,24,51</sup> the rmsds with respect to the initial A-DNA structure reach stable values of about 5 Å within 1 ns and then oscillate around it, indicating that the equilibrium of the system has been reached. The average rmsds during the last nanosecond for A1 and A2 simulations were 5.3 and 5.1 Å, respectively. The corresponding rmsds with respect to the B-DNA during the last nanosecond were 2.5 and 3.1 Å, respectively. The average structures calculated using the last nanosecond of both A1 and A2 simulations were very similar with an rmsd value of 1.42 Å between the two structures. Although the rmsd values suggest that the structure is clearly closer to B-DNA than A-DNA, the conformation is indeed intermediate between the B-DNA and the A-DNA. As pointed out by Cheatham et al.,<sup>11</sup> the rmsd value alone cannot judge A-DNA → B-DNA transition. A better way to understand whether the A-DNA has really transformed to B-DNA is to calculate two conformational parameters, the sugar pucker parameters (SP) and the minor groove width (MGW); the former determines the shape of the DNA helix by evaluating the phase angle associated with pseudorotation of the sugar rings and the latter is defined in terms of shortest interstrand P...P distances.<sup>47</sup> The average structure parameters are listed in Table 1. For A-DNA, the SP is about 0–36°, and the MGW is about 11 Å, while the corresponding values for B-DNA are 140–180° and 5.9 Å, respectively. Figure 2c shows the calculated MGW parameter as a function of the simulation time while the variation of SP against simulation time is shown in Figure 2d. For the initial conformation of the MD simulation, i.e., the optimized A-DNA, the MGW and SP values are about 11 Å and 10°, respectively (Table 2, Figure 2c,d). The conformation of DNA gradually transforms from A → B cooperatively, and the SP and MGW parameters reach their stable values during the first 500–1000 ps and then oscillate due to thermal fluctuations. It is to be noted that irrespective of the presence of [Co(NH<sub>3</sub>)<sub>6</sub>]<sup>3+</sup> ions, both A1 and A2 simulations indicate A-DNA → B-DNA transition. In the solid-state structure of the present DNA duplex,<sup>29</sup> the [Co(NH<sub>3</sub>)<sub>6</sub>]<sup>3+</sup> ions do not directly interact with the base atoms. Instead, the water molecules bridge the cobalt hexammine ions with N and O atoms of adjacent guanines and provide the requisite conformation of A-DNA. The stability of the B-DNA is known to be higher than that of A-DNA in water solution.<sup>52</sup> So it is likely that both A1 and A2 simulations would exhibit A-DNA → B-DNA transition. As apparent in Figure 2, the A → B transition is more gradual in the A1 simulation than that in the A2 simulation.

The subtle difference in the transition process during A1 and A2 simulations can be visualized by considering the interactions of [Co(NH<sub>3</sub>)<sub>6</sub>]<sup>3+</sup> ions with the DNA base pairs in the former case. In the present d(CCCGATCGGG)<sub>2</sub> duplex, the residues (5' to 3') numbering 1–10 and 12–21 correspond to the DNA

**Table 2.** Average Values Minor Groove Width and Sugar Pucker, and Energy Gap (*E<sub>g</sub>*) Values of the Representative Conformations for Simulations A1 and A2

time (ps)	A1			A2		
	MGW (Å)	SP (deg)	<i>E<sub>g</sub></i> (eV)	MGW (Å)	SP (deg)	<i>E<sub>g</sub></i> (eV)
0	11(1)	12(12)	2.3	10(1)	8(7)	2.1
100	10(1)	53(54)	2.0	9(1)	101(41)	1.9
250	9(1)	76(60)	1.7	8(1)	108(38)	1.6
500	8(1)	93(57)	2.0	7(1)	133(31)	1.8
750	7(2)	137(43)	1.3	8(2)	134(32)	1.8
1000	5(1)	140(41)	1.3	7(1)	133(40)	1.6

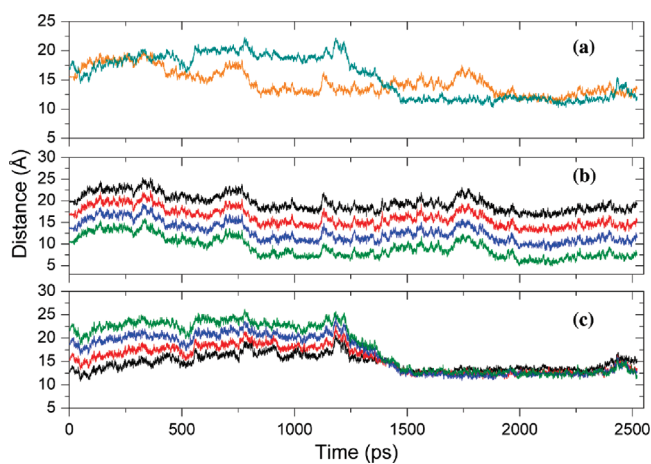


**Figure 3.** In simulation A1, the residues (5' to 3') numbering 1–10 and 12–21 correspond to the DNA fragments, and the residues 11 and 22 represent two [Co(NH<sub>3</sub>)<sub>6</sub>]<sup>3+</sup> ions. (a) The distance of the cobalt hexammine ions Co11 (orange) and Co22 (cyan) with respect to the center of mass of the DNA as a function of the simulation time. (b) Distances representing the approach from the Co11 ion to central base pairs, 4G-18C (black), 5A-17T (red), 6T-16A (blue), and 7C-15G (olive). (c) Distances representing the approach from the Co22 ion to central base pairs, 4G-18C (black), 5A-17T (red), 6T-16A (blue), and 7C-15G (olive).

fragments, and the residues 11 and 22 represent the two [Co(NH<sub>3</sub>)<sub>6</sub>]<sup>3+</sup> ions. The distances of cobalt hexammine ion pair from the center of mass of the DNA duplex during A → B transition in A1 simulation were plotted against time scale in Figure 3a, while Figure 3b,c depicts the time variation of distances of metal-amine ions from the major groove side of the central base pair. It is apparent from Figure 3a that one of the cobalt hexammine ions, Co22, changes its position abruptly during 1200–1500 ps (shown in dark cyan in Figure 3a); the other metal ion (Co11), however, remains near the G9-G10 backbone throughout the simulation process (shown in orange in Figure 3a). In the initial stages of simulation, Co11 remains in close proximity of the G9-G10 backbone, and then gradually moves toward the center of the G9-C13 and G10-C12 base pairs. This is also apparent in Figure 3b (shown in black, red, blue, and olive) where the distances of approach of Co11 to each central base pair remain relatively constant throughout the entire simulation process. The other [Co(NH<sub>3</sub>)<sub>6</sub>]<sup>3+</sup> ion (Co22), however, remained localized initially around the G20-G21 backbone of the second DNA strand and then moved upward by one residue to interact primarily with

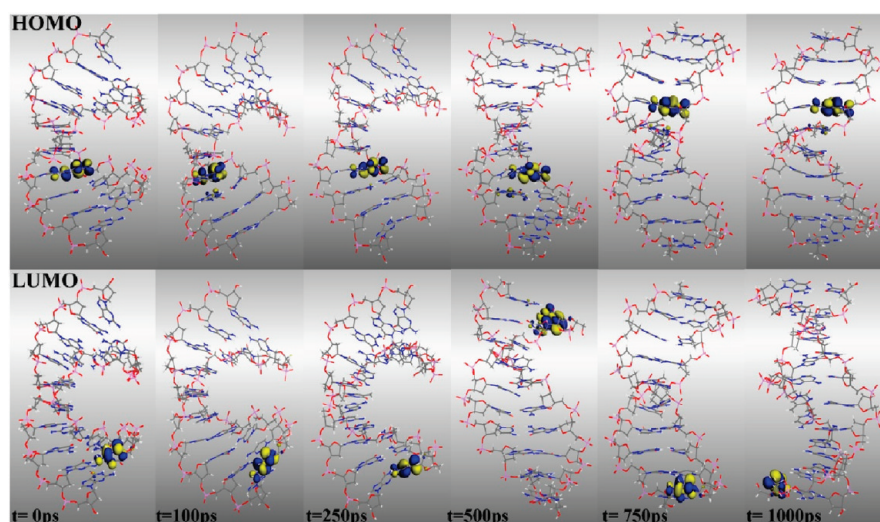


**Figure 4.** Selected representative conformations during the A  $\rightarrow$  B conformation transition process of A1; also shown are the population densities of the HOMO and LUMO for snapshots taken at the simulation time of 0, 100, 250, 500, 750, and 1000 ps.

the third guanine base, G19. During 1200–1500 ps the  $[\text{Co}(\text{NH}_3)_6]^{3+}$  ion (Co22) moves from its position around the G21-G20-G19 backbone to the center of the G4-C18 and T17-A5 base pairs. From the distances of approach of the second  $[\text{Co}(\text{NH}_3)_6]^{3+}$  ion to the central base pairs (shown in black, red, blue, and olive in Figure 3c), it is evident that the cobalt hexammine ion eventually moves into the center of the major groove side of the central base pairs. It can be concluded that as the hexammine ion moves out of the terminal GG backbone, the structure becomes closer to B-DNA. Thus, the presence of  $[\text{Co}(\text{NH}_3)_6]^{3+}$  ion bound to the GG backbone in A-DNA can account for the stability of A1 simulation.

To elucidate the effect of conformation changes, thermal fluctuations, and the presence of cobalt hexammine on the electronic properties of the DNA duplex, the electronic structure evolution during A  $\rightarrow$  B transition has been evaluated using ab initio DFT methods. A few representative conformations, which can describe the conformational change during the transition process, were selected from the nanosecond MD simulations and self-consistent calculations of each snapshot were performed. Besides the initial conformation, five intermediate steps at the time scale of 100, 250, 500, 750, and 1000 ps were considered. The corresponding SP and MGW parameters are listed in Table 2, which reveals a gradual transition from A-DNA  $\rightarrow$  B-DNA.

According to the molecular orbital theory, HOMO and LUMO are two important factors influencing the bioactivity of a system.<sup>5,14</sup> The HOMO–LUMO energy separation ( $E_g$ ) could indicate the reactivity pattern of the molecule. Since the electronic structure of DNA is related to its conformation as well as the presence of metal ions,<sup>11</sup> a gradual energy gap evolution accompanying the A  $\rightarrow$  B transition process and associated conformational parameter changes is also expected. The energy gaps ( $E_g$ ) of six representative conformations are listed in Table 2. The decrease in energy gap ( $E_g$ ) from 2.3 to 1.3 eV in A1 simulations and 2.1 to 1.6 eV in A2 simulations is also consistent with the A-DNA  $\rightarrow$  B-DNA transition in the title DNA decamer. Similar average energy gap of about 1.6 eV has been reported in the B-DNA double helix systems.<sup>14</sup> The energy gap in both simulations (Table 2), however, appears to be independent of the conformational parameters during the A  $\rightarrow$  B transition, and the

fluctuations caused by the DNA vibration play an important role during each simulation. Barton and co-workers<sup>53</sup> have emphasized the role of thermal fluctuations in determining the charge transport properties in the DNA system. Unlike most of the ab initio calculations on canonical DNA,<sup>5,6</sup> the periodic boundary condition was not adopted in our calculations since a real DNA system is not strictly periodic; i.e., the DNA was treated as a finite oligonucleotide molecule. Although the energy gaps of the DNA snapshots in our calculations are quite similar to those obtained from the infinite periodic assumption,<sup>5</sup> there exists some basic difference between the two protocols as the calculations based on the periodic structures usually give the gaps of the energy bands.

The analysis of the HOMO and LUMO distributions in natural DNA systems is important to understand their charge transport properties. The HOMO and LUMO distributions corresponding to A1 and A2 for six representative conformations are shown in Figures 4 and 5, respectively. The HOMO states are highly localized on the guanine bases, and the LUMO states are mainly populated on the phosphate groups or the base of the cytosine nucleotide. This feature is distinctly different from the extended HOMO and LUMO distributions of the periodic infinite DNA crystal.<sup>6,14</sup> The HOMO states in the DNA systems showed the so-called Anderson localization, which can be attributed to off-diagonal disorder,<sup>14</sup> a consequence of dynamical variations in DNA intramolecular interactions, and coupling of DNA with its environment. Although localized, the HOMO states occupy different guanine bases in the A1 and A2 simulations and oscillate randomly between one end of the DNA molecule and the other as time progresses. The HOMO level's localization on one guanine base is traded for localization on another guanine base through the dynamical simulation. This kind of trading reflects concerted fluctuations assignable to off-diagonal dynamical disorder in a regular homooligonucleotide duplex which is not affected by the conformational changes during the A  $\rightarrow$  B transition of the DNA molecules. The present results are consistent with the work of Taniguchi and Kawai<sup>5</sup> on the electronic structures of A-DNA and B-DNA that, irrespective of the structure type, the HOMO states are localized on the guanine bases. Similarly, the LUMO states localized on the terminal cytosine nucleotide also jump from one location to



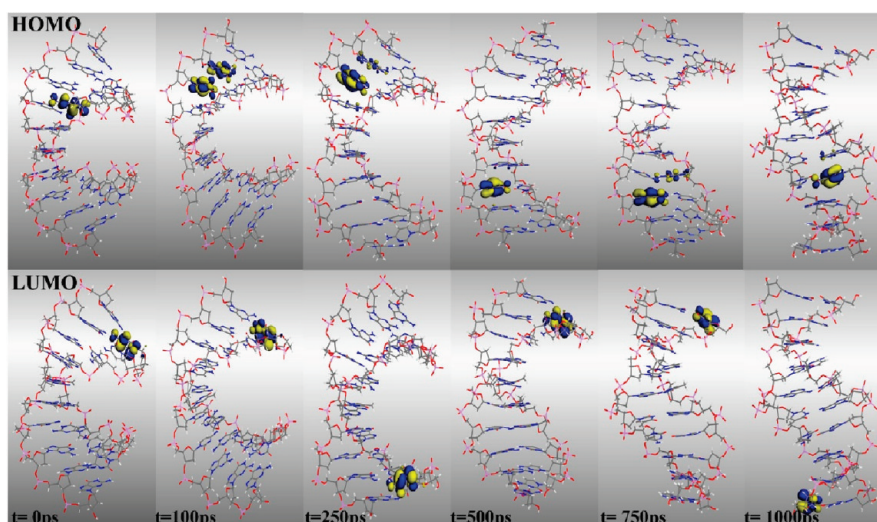


**Figure 5.** Selected representative conformations during the A  $\rightarrow$  B conformation transition process of A2; also shown are the population densities of the HOMO and LUMO for snapshots taken at the simulation time of 0, 100, 250, 500, 750, and 1000 ps.

another in both A1 and A2 simulations. The fluctuation assisting the electronic-hopping mechanism thus plays an important role in the charge transporting property of DNA duplex under dynamic condition. From the MD simulations and the electronic properties illustrated by Figures 2, 4, and 5, we conclude that the hopping of the HOMO and LUMO states in d(CCCGATCGGG)<sub>2</sub> is not a consequence of the overall conformation transition; rather, it is likely due to the thermal fluctuation of the DNA duplex. Similar phenomena of fluctuation have been reported in B-type poly(dA)-poly(dT) DNA for which no conformation transition occurs at all.<sup>14</sup>

#### 4. CONCLUSIONS

The dynamical behavior of electronic states of a decamer, d(CCCGATCGGG)<sub>2</sub>, during its transition from A  $\rightarrow$  B in the presence and absence of [Co(NH<sub>3</sub>)<sub>6</sub>]<sup>3+</sup> ions has been investigated using a combination of classical MD simulation and ab initio DFT calculations. The results indicate that the conformational parameters as well as the surrounding environment have no direct correlation with the electronic structures of the DNA duplex during its conformation transition process. The thermal fluctuations appear to play an important role in affecting the electronic structure of the DNA molecule. The highly localized HOMO and LUMO states in the DNA system randomly jump from one location to another accompanying the fluctuation process. Thus, the fluctuations assisting the electronic-hopping mechanism dominate the charge transport property in the present DNA. The HOMO states of all conformations are localized at the guanine bases, while the corresponding LUMO states are populated on the cytosine bases. The natural DNA is, however, a more complex system and its electronic structure can be influenced by many other factors. Our future efforts involve studying the effects of different sequences and environments on the evolution of the electronic structures of DNA systems.

#### AUTHOR INFORMATION

##### Corresponding Author

\*E-mail: sspmm@iacs.res.in. Tel.: +91-33-24734971 (ext 312). Fax: +91-33-2473-2805.

#### ACKNOWLEDGMENT

The authors thank Prof. A. K. Mukherjee, Department of Physics, Jadavpur University, Kolkata, and Dr. Krishna Chowdhury for their interest and for stimulating discussions.

#### REFERENCES

- (1) Ghosh, A.; Bansal, M. *Acta Crystallogr., Sect. D* **2003**, 59, 620.
- (2) Leslie, A. G.; Arnott, S.; Chandrasekaran, R.; Ratliff, R. L. *J. Mol. Biol.* **1980**, 143, 49.
- (3) Record, M. T., Jr.; Mazur, S. J.; Melançon, P.; Roe, J. H.; Shaner, S. L.; Unger, L. *Annu. Rev. Biochem.* **1981**, 50, 997.
- (4) Ohya, T., Ed. *DNA Conformation and Transcription*; Springer: New York, 2005.
- (5) Taniguchi, M.; Kawai, T. *Phys. Rev. E* **2004**, 70, 011913.
- (6) Gervasio, F. L.; Carloni, P.; Parrinello, M. *Phys. Rev. Lett.* **2002**, 89, 108102.
- (7) Klotsa, D.; Romer, R. A.; Turner, M. S. *J. Biophys.* **2005**, 89, 2187.
- (8) Tuukkanen, S.; Kuzyk, A.; Toppari, J. J.; Hytonen, V. P.; Ihalainen, T.; Torma, P. *Appl. Phys. Lett.* **2005**, 87, 183102.
- (9) Heim, T.; Melin, T.; Deresmes, D.; Vuillaume, D. *Appl. Phys. Lett.* **2004**, 85, 2637.
- (10) Xu, M. S.; Tsukamoto, S.; Ishida, S.; Kitamura, M.; Arkawa, Y.; Endres, R. G.; Shimoda, M. *Appl. Phys. Lett.* **2005**, 87, 083902.
- (11) Wang, H.; Cheatham, T. E.; Gannett, P. M.; Lewis, J. P. *Soft Matter* **2009**, 5, 685.
- (12) Song, C.; Xia, Y.; Zhao, M.; Liu, X.; Li, J.; Li, L. *Phys. Chem. Chem. Phys.* **2008**, 10, 5077.
- (13) Tsukamoto, T.; Ishikawa, Y.; Vilkas, M. J.; Natsume, T.; Dedachi, K.; Kurita, N. *Chem. Phys. Lett.* **2006**, 429, 563.
- (14) Lewis, J. P.; Cheatham, T. E.; Starikov, E. B.; Wang, T. E.; Sankey, O. F. *J. Phys. Chem. B* **2003**, 107, 2581.
- (15) O'Neill, M. A.; Barton, J. K. *J. Am. Chem. Soc.* **2004**, 126, 11471.
- (16) Valis, L.; Wang, Q.; Raytchev, M.; Buchvarov, I.; Wagenknecht, H. A.; Fiebig, T. *Proc. Natl. Acad. Sci. U.S.A.* **2006**, 103, 10192.
- (17) Cheatham, T. E.; Young, M. A. *Biopolymers* **2001**, 56, 232.
- (18) Giudice, E.; Lavery, R. *Acc. Chem. Res.* **2002**, 35, 350.
- (19) Tsukamoto, T.; Ishikawa, Y.; Dedachi, K.; Kurita, N. *Chem. Phys. Lett.* **2006**, 418, 239.
- (20) Wang, H.; Lewis, J. P. *Phys. Rev. Lett.* **2004**, 93, 016401.
- (21) Roche, S. *Phys. Rev. Lett.* **2003**, 91, 108101.
- (22) de Pablo, P. J.; Moreno-Herrero, F.; Colchero, J.; Gómez Herrero, J.; Herrero, P.; Baró, A. M.; Ordejón, P.; Soler, J. M.; Artacho, E. *Phys. Rev. Lett.* **2000**, 85, 4992.

- (23) Gervasio, F. L.; Laio, A.; Parrinello, M.; Boero, M. *Phys. Rev. Lett.* **2005**, *94*, 158103.
- (24) Cheatham, T. E.; Kollman, P. A. *J. Mol. Biol.* **1996**, *259*, 434.
- (25) Smith, D. M. A.; Adamowicz, L. *J. Phys. Chem. B* **2001**, *105*, 9345.
- (26) Voityuk, A. A.; Siri Wong, K.; Rösch, N. *Phys. Chem. Chem. Phys.* **2001**, *3*, 5421.
- (27) Troisi, A.; Orlandi, G. *J. Phys. Chem. B* **2002**, *106*, 2093.
- (28) Noy, A.; Perez, A.; Laughton, C. A.; Orozco, M. *Nucleic Acids Res.* **2007**, *35*, 3330.
- (29) Ramakrishnan, B.; Sekharudu, C.; Pan, B.; Sundaralingam, M. *Acta Crystallogr. Sect D* **2003**, *59*, 67.
- (30) Wahl, M. C.; Sundaralingam, M. *Biopolymers* **1997**, *44*, 45.
- (31) Nunn, C. M.; Neidle, S. *J. Mol. Biol.* **1996**, *256*, 340.
- (32) Gao, Y. G.; Robinson, H.; van Boom, J. H.; Wang, A. H.-J. *Biophys. J.* **1995**, *69*, 559.
- (33) Case, D. A.; Darden, T. A.; Cheatham, T. E., III; Simmerling, C. L.; Wang, J.; Duke, R. E.; Luo, R.; Merz, K. M.; Wang, B.; Pearlman, D. A.; Crowley, M.; Brozell, S.; Tsui, V.; Gohlke, H.; Mongan, J.; Hornak, V.; Cui, G.; Beroza, P.; Schafmeister, C.; Caldwell, J. W.; Ross, W. S.; Kollman, P. A. *AMBER 8*; University of California: San Francisco, CA, 2004.
- (34) Case, D. A.; Cheatham, T. E.; Darden, T.; Gohlke, H.; Luo, R.; Merz, K. M.; Onufriev, A.; Simmerling, C.; Wang, B.; Woods, R. J. *J. Comput. Chem.* **2005**, *26*, 1668.
- (35) Wang, J.; Cieplak, P.; Kollman, P. A. *J. Comput. Chem.* **2000**, *21*, 1049.
- (36) Cheatham, T. E.; Kollman, P. A. *Structure* **1997**, *5*, 1297.
- (37) Aqvist, J. *J. Phys. Chem.* **1990**, *94*, 8021.
- (38) Jorgensen, W. L.; Chandrasekhar, J.; Madura, J. D.; Impey, R. W.; Klein, M. L. *J. Chem. Phys.* **1983**, *79*, 926.
- (39) Izaguirre, J. A.; Catarello, D. P.; Wozniak, J. M.; Skeel, R. D. *J. Chem. Phys.* **2001**, *114*, 2090.
- (40) Darden, T.; York, D.; Pedersen, L. *J. Chem. Phys.* **1993**, *98*, 10089.
- (41) Ryckaert, J. P.; Ciccotti, G.; Berendsen, H. J. C. *J. Comput. Phys.* **1977**, *23*, 327.
- (42) Perez, A.; Marchan, I.; Svozil, D.; Spöner, J.; Cheatham, T. E.; Laughton, C. A.; Orozco, M. *Biophys. J.* **2007**, *92*, 3817.
- (43) Auffinger, P.; Cheatham, T. E.; Vaiana, A. C. *J. Chem. Theory Comput.* **2007**, *3*, 1851.
- (44) Shao, J.; Tanner, S. W.; Thompson, N.; Cheatham, T. E. *J. Chem. Theory Comput.* **2007**, *3*, 2312.
- (45) Beveridge, D. L.; McConnell, K. J. *Curr. Opin. Struct. Biol.* **2000**, *10*, 182.
- (46) Cheatham, T. E.; Kollman, P. A. *Annu. Rev. Phys. Chem.* **2000**, *51*, 435.
- (47) Lavery, R.; Moakher, M.; Maddocks, J. H.; Petkeviciute, D.; Zakrzewska, K. *Nucleic Acids Res.* **2009**, *37*, 5917.
- (48) Delley, B. *Phys. Rev. B* **2002**, *66*, 155125.
- (49) Perdew, J. P.; Burke, K.; Ernzerhof, M. *Phys. Rev. Lett.* **1996**, *77*, 3865.
- (50) Perdew, J. P.; Zunger, A. *Phys. Rev. B* **1981**, *23*, 5048.
- (51) Song, C.; Xia, Y.; Zhao, M.; Liu, X.; Li, F.; Ji, Y.; Huang, B.; Yin, Y. *J. Mol. Model.* **2006**, *12*, 249.
- (52) Banavali, N. K.; Roux, B. *J. Am. Chem. Soc.* **2005**, *127*, 6866.
- (53) Boon, E. M.; Barton, J. K. *Curr. Opin. Struct. Biol.* **2002**, *12*, 320.